

Photoexcitation measurement of Tan's contact for a strongly interacting Fermi gasJia Wang , Xia-Ji Liu, and Hui Hu*Centre for Quantum Technology Theory, Swinburne University of Technology, Melbourne, Victoria 3122, Australia*

(Received 8 October 2021; accepted 24 November 2021; published 13 December 2021)

We derive theoretically an exact relation between Tan's universal contact and the photoexcitation rate of a strongly interacting Fermi gas, in the case of optically transferring fermionic pairs to a more tightly bound molecular state. Our derivation generalizes the relation between Tan's contact and the closed-channel molecular fraction found earlier by Werner, Tarruell, and Castin [*Eur. Phys. J. B* **68**, 401 (2009)]. We use the relation to understand the recent low-temperature photoexcitation measurement in a strongly interacting ${}^6\text{Li}$ Fermi gas [Liu *et al.*, [arXiv:1903.12321](https://arxiv.org/abs/1903.12321)] and show that there is a reasonable agreement between theory and experiment close to the unitary limit. We propose that our relation can be applied to accurately measure Tan's contact coefficient at finite temperature in future experiments.

DOI: [10.1103/PhysRevA.104.063309](https://doi.org/10.1103/PhysRevA.104.063309)**I. INTRODUCTION**

In 2008, in a series of seminal works [1–3], Tan presented a set of elegant exact relations, showing that the short-range, large-momentum, and high-energy behaviors of a strongly correlated atomic gas, both statically and dynamically, can be universally governed by a coefficient. These relations together with the coefficient, namely Tan's relations and Tan's contact coefficient, pave an entirely new direction to understanding complicated quantum many-body systems [4–6].

To date, Tan relations have been experimentally verified in both Fermi gases [7,8] and Bose gases [9]. The key Tan's contact coefficient has also been measured in a number of ways [7,8,10–13], following different Tan relations [14–21]. In particular, great efforts have been taken to *accurately* determine the contact coefficient of a unitary Fermi gas with an infinitely large s -wave scattering length, by using Bragg spectroscopy [11,12] and radio-frequency (rf) spectroscopy [13]. At finite temperature, the measured contact of a homogeneous unitary Fermi gas clearly shows a dramatic change at the superfluid transition temperature, providing an unambiguous signature for the onset of the superfluid transition [12,13].

In this work, we would like to propose that photoexcitation, in which a fermionic pair absorbs a photon to form an excited molecule, may give an alternative, potentially more accurate method to measure a finite-temperature Tan's contact for a strongly interacting Fermi gas at the crossover from a Bose-Einstein condensate (BEC) of tightly bound dimers to a Bardeen-Cooper-Schrieffer (BCS) superfluid of loosely bound Cooper pairs [22,23]. This opens the way to experimentally determine the superfluid transition temperature at the entire BEC-BCS crossover, which remains elusive so far.

Our proposal is based on the derivation of an exact Tan relation for the photoexcitation rate, if we optically transfer fermionic pairs to a more tightly bound molecular state [24–26]. In the limit of a weak laser intensity or a small Rabi coupling, our relation recovers the known relation between

Tan's contact and the closed-channel molecular fraction, predicted earlier by Werner, Tarruell, and Castin [15]. The advantage of our relation is that it also works at a moderately large laser intensity, where the accuracy of the photoexcitation measurement could be greatly enhanced. This leads to a more accurate way to measure Tan's contact at finite temperature. As an application, we use our relation to better understand a recent photoexcitation measurement in a strongly interacting ${}^6\text{Li}$ Fermi gas at the University of Science and Technology of China (USTC), Shanghai [26]. We show that the puzzling huge discrepancy between theory and experiment, at about two orders of magnitude, can be reasonably resolved, although there is still a factor of three difference found on the BCS side at the largest magnetic field considered in the experiment.

The rest of the paper is organized as follows. In the next chapter (Sec. II), we sketch the photoexcitation scenario and present the model Hamiltonian. In Sec. III, we derive the Tan relation for the photoexcitation rate. In Sec. IV, we discuss the experimental relevance, first on analyzing the recent photoexcitation measurement and then on the proposal for future finite-temperature contact measurements. Finally, we conclude in Sec. V.

II. MODEL HAMILTONIAN

We consider the photoexcitation experiments at Rice [24], Ulm [25], and USTC Shanghai [26], all of which use a strongly interacting ${}^6\text{Li}$ Fermi gas near the Feshbach resonance at $B_0 \simeq 832.18$ G, where fermionic pairs are in the superposition with a stable, ground molecular bound state $X^1\Sigma_g^+(v=38)$. A resonant laser transition is used to photoexcite fermionic pairs in the admixture to another excited molecular bound state $A^1\Sigma_u^+(v'=68)$, which suffers from the spontaneous-emission loss at the rate γ . In the case that this is the dominant loss channel, one can determine the photoexcitation rate from the loss rate of the system, i.e., $-\dot{N}/N$.

The above-mentioned Fermi gas system can be well described by a two-channel model Hamiltonian $\mathcal{H} = \mathcal{H}_0^{(a)} + \mathcal{H}_{\text{int}}^{(a)} + \mathcal{H}^{(am)} + \mathcal{H}^{(m)}$, where [27–29]

$$\mathcal{H}_0^{(a)} = \sum_{\mathbf{k}\sigma} (\epsilon_{\mathbf{k}} - \mu) c_{\mathbf{k}\sigma}^\dagger c_{\mathbf{k}\sigma}, \quad (1)$$

$$\mathcal{H}_{\text{int}}^{(a)} = \frac{u_0}{V} \sum_{\mathbf{k}\mathbf{k}'\mathbf{q}} c_{\frac{\mathbf{q}}{2}+\mathbf{k}\uparrow}^\dagger c_{\frac{\mathbf{q}}{2}-\mathbf{k}\downarrow}^\dagger c_{\frac{\mathbf{q}}{2}-\mathbf{k}'\downarrow} c_{\frac{\mathbf{q}}{2}+\mathbf{k}'\uparrow}, \quad (2)$$

$$\mathcal{H}^{(am)} = \frac{g_0}{\sqrt{V}} \sum_{\mathbf{k}\mathbf{q}} [\phi_{g\mathbf{q}}^\dagger c_{\frac{\mathbf{q}}{2}-\mathbf{k}\downarrow} c_{\frac{\mathbf{q}}{2}+\mathbf{k}\uparrow} + \text{H.c.}], \quad (3)$$

$$\mathcal{H}^{(m)} = \sum_{\mathbf{q}} (\phi_{g\mathbf{q}}^\dagger \quad \phi_{e\mathbf{q}}^\dagger) \mathcal{M}_{\mathbf{q}} \begin{pmatrix} \phi_{g\mathbf{q}} \\ \phi_{e\mathbf{q}} \end{pmatrix} \quad (4)$$

describe respectively the kinetic Hamiltonian of atoms, the background interaction Hamiltonian of atoms with the interaction strength u_0 , the coupling between atoms and ground-state molecules (g_0), and the molecules in both ground and excited molecular states. Here, $\epsilon_{\mathbf{k}} \equiv \hbar^2 \mathbf{k}^2 / (2m)$ is the free dispersion relation, μ is the chemical potential of atoms, and $c_{\mathbf{k}\sigma}$, $\phi_{g\mathbf{q}}$, and $\phi_{e\mathbf{q}}$ are the annihilation field operators of atoms (with spin $\sigma = \uparrow, \downarrow$), ground-state molecules, and excited-state molecules, respectively. In the last Hamiltonian for molecules, $\mathcal{M}_{\mathbf{q}}$ is a 2×2 matrix,

$$\mathcal{M}_{\mathbf{q}} = \begin{bmatrix} \frac{\epsilon_{\mathbf{q}}}{2} - 2\mu + \delta_{g0} & \Omega/2 \\ \Omega/2 & \frac{\epsilon_{\mathbf{q}}}{2} - 2\mu + \delta_{e0} - \Delta - i\frac{\gamma}{2} \end{bmatrix}, \quad (5)$$

where Ω and Δ are the Rabi coupling and detuning of the photoexcitation laser, respectively, γ is loss rate, and δ_{g0} and δ_{e0} are the bare detunings of the molecular states.

The subscript “0” in various parameters indicates that these *bare* parameters are to be renormalized and related to some physical observables [28,29]. For example, u_0 will be expressed in terms of the background s -wave scattering length a_{bg} , g_0 will be replaced by the width of the Feshbach resonance W , and finally δ_{g0} and δ_{e0} will correspond to the detunings of the closed channels. The parameter renormalization has been discussed in detail in the literature [28,29]. It is very easy to implement: we can simply do the following replacements in *final* equations derived, i.e.,

$$u_0 \rightarrow u = \frac{4\pi \hbar^2}{m} a_{bg}, \quad (6)$$

$$g_0 \rightarrow g = \sqrt{\frac{4\pi \hbar^2}{m} a_{bg} W} \mu_{ag}, \quad (7)$$

$$\delta_{g0} \rightarrow \delta_g = \mu_{ag}(B - B_0), \quad (8)$$

$$\delta_{e0} \rightarrow \delta_e = \mu_{ae}(B - B_0). \quad (9)$$

For ${}^6\text{Li}$ atoms near the Feshbach resonance at $B_0 \simeq 832.18$ G, $a_{bg} \simeq -1582a_0$ ($a_0 = 0.0529177$ nm), and $W = -262.3$ G, $\mu_{ag} = 2\mu_a - \mu_g \simeq 2\mu_B$ (μ_B the Bohr magneton) is the difference in the magnetic moments of atoms and of molecules for the ground state [30], and similarly $\mu_{ae} = 2\mu_a - \mu_e \simeq 2\mu_B$. For the excited molecular state, the loss rate $\gamma \simeq 2\pi \hbar \times 11.8$ MHz. The Rabi coupling Ω is typically at the order of $2\pi \times 1.0$ MHz. In addition, to convert the Zeeman field to frequency, we could use $\mu_B \times 1$ G $\simeq 2\pi \hbar \times 1.3996$ MHz.

III. UNIVERSAL TAN RELATION FOR PHOTOEXCITATION

According to Tan, Braaten, and Platter [4], the loss rate of a quantum many-body system with short-range interparticle interactions at the number of particles N is given by

$$-\dot{N} \equiv -\frac{dN}{dt} = \frac{\hbar[-\text{Im}a(B)]}{2\pi m |a(B)|^2} \mathcal{I}. \quad (10)$$

Here, $a(B)$ is the s -wave scattering length at a given Zeeman field B and \mathcal{I} is the contact coefficient of the system. The loss rate equation can be intuitively understood from Tan’s adiabatic relation,

$$\frac{dE}{d(1/a)} = -\frac{\hbar^2}{4\pi m} \mathcal{I}, \quad (11)$$

which relates the total energy E of the many-body system to the contact coefficient \mathcal{I} . Due to the coupling to the dissipative excited molecular state, the total energy acquires a relatively small imaginary part $E - iE_1/2$, where $E_1/\hbar = -dN/dt$ can be understood as the loss rate of the system, since the time evolution of the system can be given by $\exp[-i(E - iE_1/2)t/\hbar]$. Correspondingly, the scattering length also has a small imaginary part. From the adiabatic relation, we have

$$-\frac{E_1}{2} \simeq \text{Im}[dE] = -\frac{\hbar^2 \mathcal{I}}{4\pi m} \text{Im}[d(1/a)], \quad (12)$$

which immediately leads to the loss rate equation (10).

Let us now calculate the scattering length $a(B)$ for the experimental photoexcitation process. Taking into account the molecule-mediated attraction, the total (unrenormalized) interaction between two atoms can be written into the form

$$U(\mathbf{q}, i\nu_n) = u_0 + g_0 \mathcal{D}_g^{(0)}(\mathbf{q}, i\nu_n), \quad (13)$$

where $\mathcal{D}_g^{(0)}(\mathbf{q}, i\nu_n)$ is the noninteracting Green’s function of molecules in the *ground-state* channel and is the 11 component of the 2×2 matrix,

$$\mathcal{D}^{(0)}(\mathbf{q}, i\nu_n) = [i\nu_n - \mathcal{M}_{\mathbf{q}}]^{-1}. \quad (14)$$

By explicitly working out the inverse of the matrix, we obtain that

$$\mathcal{D}_g^{(0)}(\mathbf{q}, i\nu_n) = \left[i\nu_n - \epsilon_{\mathbf{q}}/2 + 2\mu - \delta_{g0} - \frac{\Omega^2/4}{i\nu_n - \epsilon_{\mathbf{q}}/2 + 2\mu - \delta_{e0} + \Delta + i\gamma/2} \right]^{-1}. \quad (15)$$

The last term in the bracket gives the conventional Stark shift to the ground-state molecules due to the coupling to the excited molecular state. In the vacuum, where we set the chemical potential $\mu = 0$, the s -wave scattering length $a(B)$ is then given by

$$\frac{4\pi \hbar^2 a(B)}{m} = u_0 + g_0^2 \mathcal{D}_g^{(0)}(\mathbf{0}, 0) \quad (16)$$

$$= u - \frac{g^2}{\delta_g + \Omega^2/[4(-\delta_e + \Delta + i\gamma/2)]}. \quad (17)$$

In the last step, we have replaced the unregularized parameters with the regularized ones. In the absence of the Rabi coupling, i.e., $\Omega = 0$, it is easy to check that we recover the well-known expression for the scattering length near a Feshbach resonance,

$$a_s(B) = \frac{m}{4\pi\hbar^2} \left[u - \frac{g^2}{\delta_g} \right] = a_{bg} \left(1 - \frac{W}{B - B_0} \right). \quad (18)$$

Here, the subscript “s” in $a_s(B)$ indicates the s -wave scattering length *without* Rabi coupling. In the presence of Rabi coupling, instead we would obtain

$$a(B) = a_{bg} - \frac{a_{bg}\Gamma}{\delta_g + \Omega^2/[4(-\delta_e + \Delta + i\gamma/2)]}, \quad (19)$$

where $\Gamma \equiv \mu_{ag}W$ is the characteristic energy related to the width of the Feshbach resonance. It is straightforward to obtain

$$-\frac{\text{Im}a(B)}{|a(B)|^2} = \left(\frac{\Gamma}{a_{bg}} \right) \frac{[\Omega^2/(2\gamma)]}{(\delta_g - \Gamma)^2 + c^2[\Omega^2/(2\gamma)]^2}, \quad (20)$$

where the coefficient

$$c = 1 - \frac{4(\delta_e - \Delta)(\delta_g - \Gamma)}{\Omega^2}. \quad (21)$$

By substituting it into the loss rate expression (10), we find that

$$-\frac{\dot{N}}{N} = \frac{\hbar\mathcal{I}}{2\pi mN} \left(\frac{\Gamma}{a_{bg}} \right) \frac{[\Omega^2/(2\gamma)]}{(\delta_g - \Gamma)^2 + c^2[\Omega^2/(2\gamma)]^2}. \quad (22)$$

By recalling that

$$\delta_g - \Gamma = -\frac{\Gamma}{[1 - a_{bg}/a_s]}, \quad (23)$$

and defining [15]

$$R_* = \frac{\hbar^2}{ma_{bg}\Gamma}, \quad (24)$$

$$\mathcal{I} = 4\pi N k_F \mathcal{F} \left(\frac{1}{k_F a_s} \right), \quad (25)$$

we finally arrive at

$$-\frac{\dot{N}}{N} = \hbar^{-1} k_F R_* \mathcal{F} \left(\frac{1}{k_F a_s} \right) L(\Delta), \quad (26)$$

where the line-shape function of the photoexcitation laser $L(\Delta)$ takes the form

$$L(\Delta) = \frac{\Omega^2/\gamma}{[1 - a_{bg}/a_s]^{-2} + \left[\frac{\Omega^2 - 4(\delta_e - \Delta)(\delta_g - \Gamma)}{2\gamma\Gamma} \right]^2}. \quad (27)$$

Under the resonant condition $\delta_e = \Delta$ and with a weak laser intensity $\Omega^2 \ll \gamma\Gamma$, the line-shape function is $L(\Delta) = (1 - a_{bg}/a_s)^2 \Omega^2/\gamma$. As $\hbar^{-1}\Omega^2/\gamma$ is the effective decay rate of the ground molecular state for a resonant transition, see, i.e., Eq. (15), we may rewrite [24,26]

$$-\frac{\dot{N}}{N} = Z \frac{\Omega^2}{\hbar\gamma}, \quad (28)$$

where Z is the molecular fraction in the ground molecular state and hence is given by

$$Z = k_F R_* \mathcal{F} \left(\frac{1}{k_F a_s} \right) \left[1 - \frac{a_{bg}}{a_s} \right]^2 = \frac{\mathcal{I} R_*}{4\pi N} \left[1 - \frac{a_{bg}}{a_s} \right]^2. \quad (29)$$

Thus, in the limit of a weak laser intensity, we recover the universal relation that links the closed-channel molecular fraction to the contact coefficient, first pointed out by Werner *et al.* [15]. Our loss rate equation (26) does not have the weak probe restriction. It holds as long as the assumption of a single s -wave scattering length $a_s(B)$ is applicable.

IV. EXPERIMENTAL RELEVANCE

A. Photoexcitation measurement at USTC Shanghai

In a recent experiment at USTC Shanghai [26], the laser intensity is weak and the Rabi coupling is measured to be $\Omega^2/\gamma \simeq 2\pi\hbar \times 0.136(1)$ MHz. This is much smaller than the characteristic energy of the Feshbach resonance width, i.e., $\Gamma = \mu_{ag}W = 2\mu_B \times 262.3$ G $\simeq 2\pi\hbar \times 734$ MHz. Therefore, for resonant excitation ($\delta_e = \Delta$) we may use the weak-intensity result,

$$-\frac{\dot{N}}{N} = k_F R_* \mathcal{F} \left(\frac{1}{k_F a_s} \right) \left[1 - \frac{a_{bg}}{a_s} \right]^2 \left(\frac{\Omega^2}{\hbar\gamma} \right), \quad (30)$$

to analyze the experimental data and to calculate the closed-channel fraction Z in the ground molecular state according to Eq. (29). In Fig. 1, we present the density dependence of the closed-channel fraction Z in the unitary limit $B = 832$ G (a) and on the BCS side $B = 925$ G (b), experimentally measured at USTC Shanghai [26] and theoretically calculated by using Eq. (29) with the contact obtained either from a Gaussian pair-fluctuation theory [20,31,32] or from a perturbation theory [15]. The latter is only applicable in the deep BCS limit. We find a good agreement between theory and experiment in the unitary limit. However, on the BCS side, there is about a factor of three difference. In Fig. 2, we show the comparison as a function of the magnetic field. The agreement seems to become increasingly worse when we increase the magnetic field.

We do not fully understand why there is about a factor of three difference on the BCS side. A possible source for the discrepancy is the Rabi coupling Ω , which is only experimentally calibrated on the BEC side and is then assumed to be *invariant* across the BEC-BCS crossover. Mathematically, the Rabi coupling is given by the overlap between the two wave functions of the bound molecular states [24], i.e.,

$$\Omega = \langle \psi_{v'=68}(S=0) | \vec{d} \cdot \vec{E}_L | \psi_{v=38}(S=0) \rangle, \quad (31)$$

where \vec{d} is the transition dipole and \vec{E}_L is the laser field for photon excitation. This wave-function overlap could change notably on the BCS side, as the ground molecular state becomes increasingly affected by the admixture with atoms. A few-body calculation is needed, i.e., following the theoretical photoassociation work [33], in order to fully understand the magnetic dependence of the Rabi coupling near a Feshbach resonance.

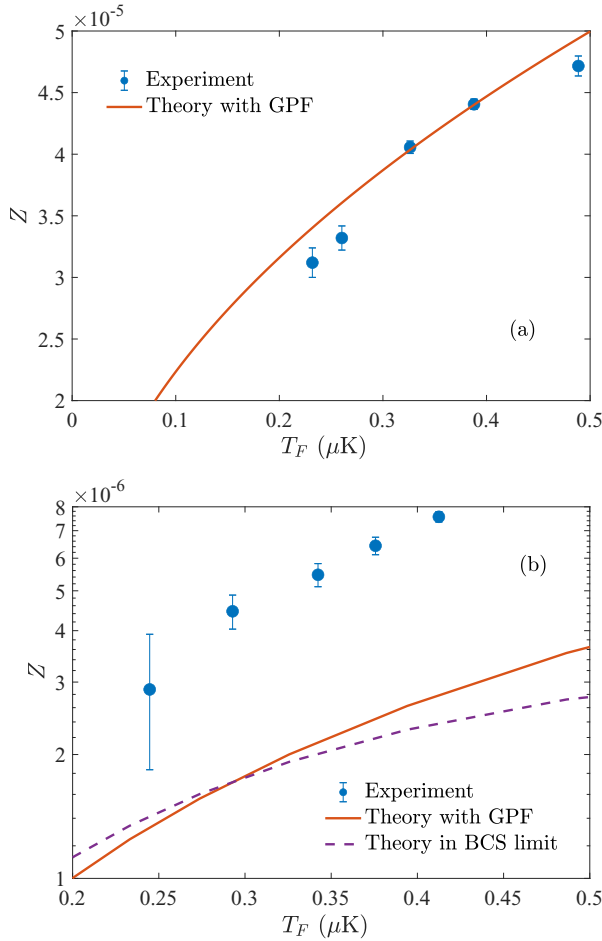


FIG. 1. Density dependence of the closed-channel fraction Z of a strongly interacting ${}^6\text{Li}$ Fermi gas in the unitary limit $B = 832$ G (a) and on the BCS side at the magnetic field $B = 925$ G. Here, the density is expressed in terms of the Fermi energy T_F . The low-temperature data from USTC Shanghai group (symbols) [26] are compared with our zero-temperature theoretical predictions using the contact obtained from a Gaussian pair fluctuation theory (solid line) [20] and a perturbation theory (dashed line) [15].

B. Contact measurement at finite temperature

To avoid the complications due to the magnetic field dependence in the Rabi coupling, we may perform the photoexcitation measurement at a fixed magnetic field and consider different temperatures. To calibrate Ω^2/γ , we can go to the strong laser intensity regime, in the sense that Ω^2/γ can be enlarged to be comparable to Γ , as long as there is no significant heating. This will considerably increase the experimental resolution for the loss rate measurement.

In greater detail, by increasing the laser intensity I to increase the Rabi coupling (i.e., $\Omega^2 = \alpha I$), under the resonant condition we may first confirm the predicted line shape in Eq. (27),

$$L(\Delta) = 2\Gamma \frac{\Omega^2/(2\gamma\Gamma)}{[1 - a_{bg}/a_s]^{-2} + [\Omega^2/(2\gamma\Gamma)]^2}, \quad (32)$$

which takes a maximum $2\Gamma(1 - a_{bg}/a_s)$. At a given magnetic field, the detunings Δ , δ_g , δ_e , and $a_s(B)$ are known precisely

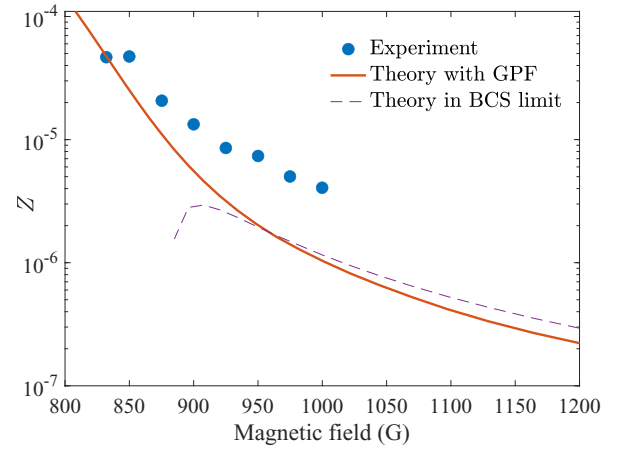


FIG. 2. Magnetic-field dependence of the closed-channel fraction Z of a strongly interacting ${}^6\text{Li}$ Fermi gas at the density characterized by a Fermi temperature $T_F = 0.45$ μK . The low-temperature data from USTC Shanghai group (symbols) [26] are compared with our zero-temperature theoretical predictions using the contact obtained from a Gaussian pair fluctuation theory (solid line) [20] and a perturbation theory (dashed line) [15].

and the zero-temperature contact has been also determined to a reasonable accuracy. Using this knowledge, we can determine the proportional factor α and hence calibrate the Rabi coupling Ω . Then, working at a fixed Rabi coupling, we may tune the temperature of the system and consequently measure the temperature dependence of the contact coefficient. As the contact coefficient changes significantly across the superfluid phase transition, we can ultimately determine the critical temperature of a strongly interacting Fermi gas across the BEC-BCS crossover.

V. CONCLUSIONS

In summary, we have derived a universal relation for the photon-excitation measurement of a strongly interacting Fermi gas near a Feshbach resonance. We have shown that the determination of the photoexcitation rate can directly give Tan's contact coefficient. In the limit of a weak laser intensity, our relation reduces to the well-known relation for the closed-channel molecular fraction, derived earlier by Werner, Tarruell, and Castin [15]. With a strong laser intensity, we anticipate that the photon-excitation measurement can have improved experimental resolution and hence provide an accurate way to measure the temperature dependence of the contact coefficient and also the critical temperature at the BEC-BCS crossover.

ACKNOWLEDGMENTS

We thank Y.-A. Chen, Q. Chen, X.-C. Yao, and J. Hecker Denschlag for the stimulating discussions. This research was supported by the Australian Research Council's (ARC) Discovery Program, Grants No. DE180100592 and No. DP190100815 (J.W.), Grant No. DP170104008 (H.H.), and Grant No. DP180102018 (X.-J.L.).

- [1] S. Tan, Energetics of a strongly correlated Fermi gas, *Ann. Phys. (NY)* **323**, 2952 (2008).
- [2] S. Tan, Large momentum part of a strongly correlated Fermi gas, *Ann. Phys. (NY)* **323**, 2971 (2008).
- [3] S. Tan, Generalized virial theorem and pressure relation for a strongly correlated Fermi gas, *Ann. Phys. (NY)* **323**, 2987 (2008).
- [4] E. Braaten and L. Platter, Exact Relations for a Strongly Interacting Fermi Gas from the Operator Product Expansion, *Phys. Rev. Lett.* **100**, 205301 (2008).
- [5] S. Zhang and A. J. Leggett, Universal properties of the ultracold Fermi gas, *Phys. Rev. A* **79**, 023601 (2009).
- [6] R. Combescot, F. Alzetto, and X. Leyronas, Particle distribution tail and related energy formula, *Phys. Rev. A* **79**, 053640 (2009).
- [7] J. T. Stewart, J. P. Gaebler, T. E. Drake, and D. S. Jin, Verification of Universal Relations in a Strongly Interacting Fermi Gas, *Phys. Rev. Lett.* **104**, 235301 (2010).
- [8] E. D. Kuhnle, H. Hu, X. J. Liu, P. Dyke, M. Mark, P. D. Drummond, P. Hannaford, and C. J. Vale, Universal Behavior of Pair Correlations in a Strongly Interacting Fermi Gas, *Phys. Rev. Lett.* **105**, 070402 (2010).
- [9] R. J. Wild, P. Makotyn, J. M. Pino, E. A. Cornell, and D. S. Jin, Measurements of Tan's Contact in an Atomic Bose-Einstein Condensate, *Phys. Rev. Lett.* **108**, 145305 (2012).
- [10] Y. Sagi, T. E. Drake, R. Paudel, and D. S. Jin, Measurement of the Homogeneous Contact of a Unitary Fermi Gas, *Phys. Rev. Lett.* **109**, 220402 (2012).
- [11] S. Hoinka, M. Lingham, K. Fenech, H. Hu, C. J. Vale, J. E. Drut, and S. Gandolfi, Precise Determination of the Structure Factor and Contact in a Unitary Fermi Gas, *Phys. Rev. Lett.* **110**, 055305 (2013).
- [12] C. Carcy, S. Hoinka, M. G. Lingham, P. Dyke, C. C. N. Kuhn, H. Hu, and C. J. Vale, Contact and Sum Rules in a Near-Uniform Fermi Gas at Unitarity, *Phys. Rev. Lett.* **122**, 203401 (2019).
- [13] B. Mukherjee, P. B. Patel, Z. Yan, R. J. Fletcher, J. Struck, and M. W. Zwierlein, Spectral Response and Contact of the Unitary Fermi Gas, *Phys. Rev. Lett.* **122**, 203402 (2019).
- [14] M. Punk and W. Zwerger, Theory of rf-Spectroscopy of Strongly Interacting Fermions, *Phys. Rev. Lett.* **99**, 170404 (2007).
- [15] F. Werner, L. Tarruell, and Y. Castin, Number of closed-channel molecules in the BEC-BCS crossover, *Eur. Phys. J. B* **68**, 401 (2009).
- [16] E. Braaten, D. Kang, and L. Platter, Short-Time Operator Product Expansion for rf Spectroscopy of a Strongly Interacting Fermi Gas, *Phys. Rev. Lett.* **104**, 223004 (2010).
- [17] E. Taylor and M. Randeria, Viscosity of strongly interacting quantum fluids: Spectral functions and sum rules, *Phys. Rev. A* **81**, 053610 (2010).
- [18] D. T. Son and E. G. Thompson, Short-distance and short-time structure of a unitary Fermi gas, *Phys. Rev. A* **81**, 063634 (2010).
- [19] H. Hu, X.-J. Liu, and P. D. Drummond, Static structure factor of a strongly correlated Fermi gas at large momenta, *Europhys. Lett.* **91**, 20005 (2010).
- [20] H. Hu, X. J. Liu, and P. D. Drummond, Universal contact of strongly interacting fermions at finite temperatures, *New J. Phys.* **13**, 035007 (2011).
- [21] H. Hu and X.-J. Liu, Universal dynamic structure factor of a strongly correlated Fermi gas, *Phys. Rev. A* **85**, 023612 (2012).
- [22] S. Giorgini, L. P. Pitaevskii, and S. Stringari, Theory of ultracold atomic Fermi gases, *Rev. Mod. Phys.* **80**, 1215 (2008).
- [23] M. Randeria and E. Taylor, Crossover from Bardeen-Cooper-Schrieffer to Bose-Einstein condensation and the unitary fermi gas, *Annu. Rev. Condens. Matter Phys.* **5**, 209 (2014).
- [24] G. B. Partridge, K. E. Strecker, R. I. Kamar, M. W. Jack, and R. G. Hulet, Molecular Probe of Pairing in the BEC-BCS Crossover, *Phys. Rev. Lett.* **95**, 020404 (2005).
- [25] T. Paintner, D. K. Hoffmann, M. Jäger, W. Limmer, W. Schoch, B. Deissler, M. Pini, P. Pieri, G. C. Strinati, C. Chin, and J. H. Denschlag, Pair fraction in a finite-temperature Fermi gas on the BEC side of the BCS-BEC crossover, *Phys. Rev. A* **99**, 053617 (2019).
- [26] X.-P. Liu, X.-C. Yao, H.-Z. Chen, X.-Q. Wang, Y.-X. Wang, Y.-A. Chen, Q. Chen, K. Levin, and J.-W. Pan, Observation of the density effect on the closed-channel fraction in a ${}^6\text{Li}$ superfluid, [arXiv:1903.12321](https://arxiv.org/abs/1903.12321).
- [27] Y. Ohashi and A. Griffin, BCS-BEC Crossover in a Gas of Fermi Atoms with a Feshbach Resonance, *Phys. Rev. Lett.* **89**, 130402 (2002).
- [28] G. M. Falco and H. T. C. Stoof, Atom-molecule theory of broad Feshbach resonances, *Phys. Rev. A* **71**, 063614 (2005).
- [29] X.-J. Liu and H. Hu, Self-consistent theory of atomic Fermi gases with a Feshbach resonance at the superfluid transition, *Phys. Rev. A* **72**, 063613 (2005).
- [30] G. Zürn, T. Lompe, A. N. Wenz, S. Jochim, P. S. Julienne, and J. M. Hutson, Precise Characterization of ${}^6\text{Li}$ Feshbach Resonances Using Trap-Sideband-Resolved RF Spectroscopy of Weakly Bound Molecules, *Phys. Rev. Lett.* **110**, 135301 (2013).
- [31] H. Hu, X.-J. Liu, and P. D. Drummond, Equation of state of a superfluid Fermi gas in the BCS-BEC crossover, *Europhys. Lett.* **74**, 574 (2006).
- [32] H. Hu, P. D. Drummond, and X.-J. Liu, Universal thermodynamics of strongly interacting Fermi gases, *Nat. Phys.* **3**, 469 (2007).
- [33] P. Pellegrini, M. Gacesa, and R. Côté, Giant Formation Rates of Ultracold Molecules via Feshbach-Optimized Photoassociation, *Phys. Rev. Lett.* **101**, 053201 (2008).